Int. J. Heat Mass Transfer. Vol. 36, No. 7, pp. 1897–1904, 1993
Printed in Great Britain

0017–9310/93 $6.00 + 0.00

Convective instability in saturated porous enclosures with a vertical insulating baffle

FALIN CHEN and C. Y. WANG†
Institute of Applied Mechanics, National Taiwan University, Taipei, Taiwan 10764, R.O.C.

(*Received* 20 *June* 1992 *and in final form* 8 *September* 1992)

Abstract—The convective instability in two-dimensional enclosures containing a fluid-saturated porous medium with an insulating baffle extending vertically from the bottom boundary is investigated. The baffle influences the stability through its height and its horizontal position. It is found, in general, that a taller baffle does not necessarily result in a more stable state, the optimum height of the baffle changes as its position varies; a baffle located at the middle or at a position with $\lambda = \sqrt{(k(k+1))}$, $k = 1, 2, \ldots$, where λ accounts for the normalized distance from the baffle to the left wall, corresponds to a relatively more stable state; while a baffle coinciding with a dividing streamline has no influence on the stability. These findings are concluded on the basis of the results obtained by a linear stability analysis covering a wide range of relevant parameters and are believed to be applicable to some engineering designs, such as the insulating systems for building and heat exchangers.

1. INTRODUCTION

BUOYANCY-driven natural convection in enclosures containing a fluid-saturated porous medium has received much attention recently because the data concerning buoyant enclosure flow are in great demand for many traditional and contemporary applications such as insulating systems for buildings and heat exchanger devices, energy storage systems, material processing and geothermal systems. Reviews of previous works and applications are provided by, for example, Cheng [1] and Bejan [2]. Another reason leading to study of the convection in porous medium enclosures is the interest in fundamental phenomena of instability and transition of the convective flow. Due to the simplicity of geometry as well as the thermal boundary conditions, the base solutions for velocity and temperature fields are so readily available that their instabilities and the subsequent flow transitions, which may eventually end up with a turbulent flow, can be more easily studied (see Caltagirone [3], Horne and Caltagirone [4], Steen and Aidun [5], and Stamps *et al.* [6]).

The natural convection in a horizontally infinite porous layer bounded above and below by two isothermal rigid plates has been studied by Horton and Rogers [7]. By utilizing a linear stability analysis, they were able to determine the critical Rayleigh number, based on the depth and permeability of the porous layer, to be $4\pi^2$ for the onset of convection from a quiescent conduction state. Later, experiments were conducted by numerous investigators to verify this criterion, for example, Katto and Masuoka [8], Buretta [9], and Chen and Chen [10]. The infinite-layer results are expected to be good approximations to those of confined enclosures of large aspect ratios σ (width to height). As σ decreases, nevertheless, the presence of two vertical side walls will significantly influence the stability as well as the bifurcation characteristics of convection [3, 11]. As a consequence, the physical phenomena of convective flow becomes increasingly complex and the critical Rayleigh numbers for the onset of convection as well as the onset of bifurcation differ considerably from those to the infinite-layer case.

In order to study from another perspective the influence of the presence of a vertical wall on the convective instability in a porous medium, we consider two-dimensional enclosures in which a vertical partition is introduced (Fig. 1). The vertical partition, or baffle, can either completely or partially divide the enclosure into two compartments depending on the value of β, the height of the baffle normalized by the height of the enclosure. For $\beta = 0$, the baffle does not exist. For $\beta = 1$, the baffle divides the enclosure into two separated compartments. For $0 < \beta < 1$, the baffle partially divides the enclosure into two regions, which are connected to each other through the gap between the tip of the baffle and the top boundary. As a result of introducing the vertical baffle, the convective flow patterns are no longer simple rectangular-like cells as usually seen in either the infinite-layer case or in the case of a confined enclosure without baffle. The change of the flow pattern is associated with the change of convective stability as well as the resultant heat transfer. The main purpose of the present paper

† On leave from Michigan State University, East Lansing, MI 48824, U.S.A.

NOMENCLATURE

B	coefficient, equations (12) and (13)
C	coefficient, equations (15) and (16)
F	characteristic function, equation (17)
g	gravitational acceleration constant
H	height of enclosure
K	permeability
M	number of cells in horizontal direction
N	number of collocation point
p	pressure
R	Rayleigh number
T	temperature
u	horizontal velocity
v	vertical velocity
x	horizontal coordinate
y	vertical coordinate.

Greek symbols

α	thermal expansion coefficient
β	normalized height of baffle
κ	thermal diffusivity
λ	normalized distance from baffle to left wall
μ	viscosity
ρ	density
σ	aspect ratio, width to height
ϕ	equations (10) and (14)
ψ	stream function.

Superscripts

$'$	dimensional total quantity
c	critical value.

Subscripts

l	upper boundary
h	lower boundary
n	number in series
x	$\partial/\partial x$
y	$\partial/\partial y$
0	reference value
1	left region
2	right region.

is to investigate the variation of the stability characteristics, in terms of the critical Rayleigh number as well as the critical flow patterns, due to the presence of a vertical baffle.

2. PROBLEM FORMULATION AND METHOD OF SOLUTION

Figure 1 shows the situation. A rectangular box of height H and width σH is filled with a fluid-saturated porous medium. A vertical baffle of height βH ($0 \leqslant \beta \leqslant 1$) is located at a distance of λH from the left wall. The side walls and the baffle are adiabatic. The top and bottom walls are isothermal and at temperatures T_l and T_h ($> T_l$), respectively. The limiting case $\beta = 0$, in which the vertical baffle had vanished and its corresponding convective stability had been discussed by, for instance, Caltagirone [3], will be discussed in Section 3. It is assumed that the Darcy–Boussinesq model governs the flow in the porous medium and the principle of exchange of instabilities holds for the present situation [12, 13]. The Darcy–Boussinesq model is applicable in a wide variety of porous media, in which the permeability ranges from approximately 10^{-3} to 10^{-6}, and we choose 10^{-4} for the present analysis.

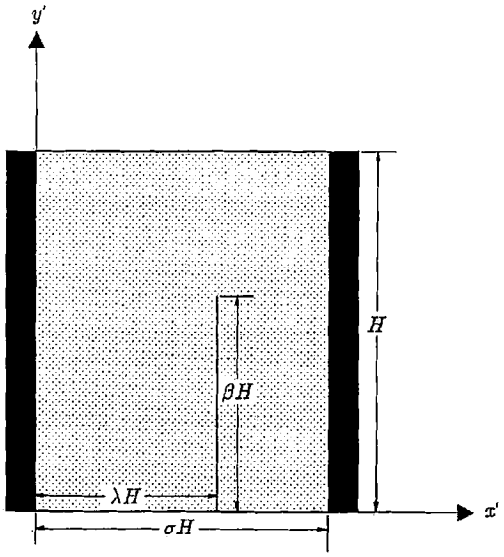

FIG. 1. Schematic description of the physical problem.

Let u' and v' be the velocity components in the x' and y' directions, respectively. The governing equations are [14]

$$u' = -\frac{K}{\mu} p'_{x'} \tag{1}$$

$$v' = -\frac{K}{\mu} \{p'_{y'} + \rho_0 g[1-\alpha(T'-T_l)]\} \tag{2}$$

$$u'T'_{x'} + v'T'_{y'} = \kappa(T'_{x'x'} + T'_{y'y'}) \tag{3}$$

$$u'_{x'} + v'_{y'} = 0. \tag{4}$$

Here K is the permeability, μ the dynamic viscosity, p the pressure, ρ_0 the fluid density at temperature T_l, g the gravitational acceleration, α the thermal expansion coefficient, T' the temperature and κ the effective thermal diffusivity of the porous medium being defined as $\kappa = \kappa_f\phi + \kappa_s(1-\phi)$, where κ_f and κ_s are the thermal diffusivity of the liquid and the solid, respectively, and ϕ the porosity of the porous medium. We perturb

from the state of pure conduction and nondimensionalize the linearized equations by the scales $T' = T_h - \Delta T(y-T)$, $u' = \kappa u/H$, $v' = \kappa v/H$, $x' = Hx$, and $y' = Hy$, where $\Delta T = T_h - T_l$. After pressure is eliminated, the linearized equations are

$$u_y - v_x = -RT_x \tag{5}$$

$$-v = T_{xx} + T_{yy} \tag{6}$$

$$u_x + v_y = 0 \tag{7}$$

where R is the Rayleigh number defined as $R = K\alpha\rho_0 gH\Delta T/\mu\kappa$. After introduction of a stream function ψ satisfying $u = \psi_y$, $v = -\psi_x$, one obtains

$$\nabla^2\psi = -RT_x, \quad \psi_x = \nabla^2 T. \tag{8}$$

These two equations can be combined into

$$\nabla^4\psi + R\psi_{xx} = 0. \tag{9}$$

Equation (9) is to be solved with the boundary conditions that ψ and ψ_{yy} be zero on the top and bottom boundaries, and ψ and ψ_{xx} be zero on the baffle and the side walls. The condition $\psi_{yy} = 0$ on the horizontal boundaries is due to the constant temperature condition $T = 0$ along the boundaries, which in turn leads to $T_x = 0$ and thus $\psi_{yy} = 0$ according to equation (8). Similar derivation applies for $\psi_{xx} = 0$ for the vertical boundaries including the baffle. At the intersection of the vertical baffle and the horizontal bottom boundary the condition $\psi_{yy} = 0$ is prescribed. The lowest eigenvalue of R for which nontrivial ψ exists is the critical Rayleigh number R^c.

Due to the presence of the baffle, the determination of R^c as the function of σ, β and λ is no longer valid by using the normal mode analysis. We hence present a method utilizing eigenfunction expansion and collocation to solve the problem. We first separate the enclosure into two regions by a vertical straight line along the baffle. Let ψ_1 be the solution to the left region and ψ_2 the solution to the right region. In the left region, the general solution of ψ_1 can be expressed by the following series

$$\psi_1(x,y) = \sum_{n=1}^{\infty} \sin(n\pi y)\phi_{1n}(x). \tag{10}$$

By substituting equation (10) into equation (9), one finds that ϕ_{1n} satisfies

$$\phi_{1n}'''' + (R - 2n^2\pi^2)\phi_{1n}'' + n^4\pi^4\phi_{1n} = 0. \tag{11}$$

The boundary conditions $\psi_1(0,y) = \psi_{1xx}(0,y) = 0$ yield two forms of ϕ_{1n} for different values of R. For $R < 4n^2\pi^2$, ϕ_{1n} is expressed as

$$\phi_{1n} = B_{1n}\cosh(ax)\sin(bx) + B_{2n}\sinh(ax)\cos(bx) \tag{12}$$

where $a = \sqrt{(n^2\pi^2 - R/4)}$, $b = \sqrt{(R/4)}$. For $R \geqslant 4n^2\pi^2$, ϕ_{1n} becomes

$$\phi_{1n} = B_{1n}\sin(cx) + B_{2n}\sin(dx) \tag{13}$$

where $c = \sqrt{(R/4)} + \sqrt{(R/4 - n^2\pi^2)}$, and $d = \sqrt{(R/4)} - \sqrt{(R/4 - n^2\pi^2)}$.

Similarly for the right region the stream function ψ_2 can be written as

$$\psi_2(x,y) = \sum_{n=1}^{\infty} \sin(n\pi y)\phi_{2n}(x) \tag{14}$$

where if $R < 4n^2\pi^2$

$$\phi_{2n} = C_{1n}\cosh[a(x-\sigma)]\sin[b(x-\sigma)] + C_{2n}\sinh[a(x-\sigma)]\cos[b(x-\sigma)] \tag{15}$$

and if $R \geqslant 4n^2\pi^2$

$$\phi_{2n} = C_{1n}\sin[c(x-\sigma)] + C_{2n}\sin[d(x-\sigma)]. \tag{16}$$

Since ψ_1 and ψ_2 are to satisfy mixed boundary conditions along the dividing line at $x = \lambda$, the boundary conditions for $0 \leqslant y \leqslant \beta$ are that the stream functions and their second horizontal derivative vanish; while for $\beta < y \leqslant 1$, the stream functions and their first three horizontal derivatives are continuous. We take a finite number of terms, say $n = 1$–N in the series represented by equations (10) and (14). This gives N interior points, evenly spaced, along $0 < y < 1$, $x = \lambda$. In order to obtain nontrivial values of B's and C's, the determinant of the coefficient matrix of $4N$ by $4N$ is set to zero, yielding a characteristic equation

$$F(R, \sigma, \lambda, \beta) = 0. \tag{17}$$

Equation (17) is nonlinear and will be solved numerically for the smallest R (R^c). Regarding σ, β and λ as being known *a priori*, the eigenvalue R^c of equation (17) is sought using a bisection algorithm.

3. RESULTS AND DISCUSSION

To determine the required number of collocation points as well as the number of terms (N) in series of equations (10) and (14) for yielding an accurate solution, we compute the R^c for $\beta = 0$, for which the exact solution can be obtained from equation (17) as follows [11]

$$R^c = 2\pi^2 + \left(\frac{M\pi}{\sigma}\right)^2 + \frac{\pi^4}{\left(\frac{M\pi}{\sigma}\right)^2} \tag{18}$$

where $\sqrt{(M(M-1))} \leqslant \sigma \leqslant \sqrt{(M(M+1))}$ and M accounts for the number of cells in the horizontal direction. It is found that the calculated R^c differs from the exact solution of equation (18) by less than 0.01% when $N = 50$ is used. We thus use $N = 50$ for the subsequent calculations in this paper. We note that the minimum of R^c ($=4\pi^2$) occurs at integer values of σ and the local maximum occurs at $\sigma = \sqrt{2}$, $\sqrt{6}$, $\sqrt{(12)}$, $\sqrt{(20)}$, $\sqrt{(30)}$, and so on. We shall call these σ corresponding to the local maximum of R^c the nodal values.

To examine the influence of the baffle on the stability characteristics, we first focus on the case of a baffle

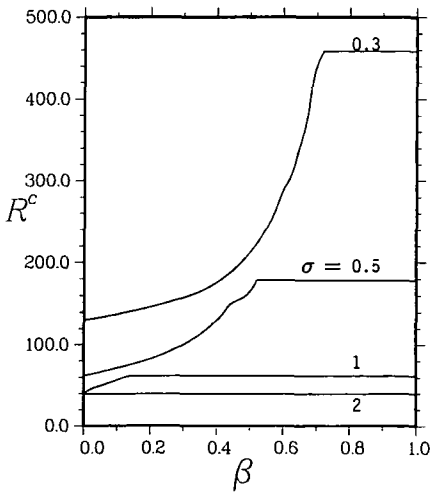

FIG. 2. Variation of R^c vs β for various σ when $\lambda/\sigma = 0.5$.

extending vertically from the middle of the bottom boundary, i.e. the centered baffle case. The variations of R^c vs β for different σ are shown in Fig. 2. For $\sigma = 0.3$, R^c increases monotonically with β first, reaches a constant ($R^c = 458.63$) at aproximately $\beta = 0.71$ and remains at the same value for larger β. The constant R^c for $\beta > \beta^c$, the critical value at which R^c reaches the maximum, means baffles of sufficient height have the same effect on the stability as totally partitioning the enclosure. For $\sigma = 0.5$ and 1, similar trends for R^c varying with β are found and the β^c are approximately 0.51 and 0.13, respectively. The maximum values of R^c for $\sigma = 0.5$ and 1 are, respectively, 178.27 and 61.68. For $\sigma = 2$, the presence of the centered-baffle does not influence the stability since R^c remains constant (39.48) for all the β considered.

To gain physical insights into the onset of instability, we present the critical streamline patterns for the case of $\sigma = 0.5$. The streamline patterns shown in the figures account for the flow which occurs at the onset of convection, where the quantity is negligibly small due to the consideration of small disturbance. The flow pattern at onset, however, is likely to sustain to some extent in the nonlinear regime for most of the convective flow and thus can be representative for the convection of the system. Figures 3(a)–(h) illustrate the critical streamline patterns for $\lambda = 0.25$ and β varying from 0 to 0.6. For $\beta = 0$ (Fig. 3(a)), a unicellular convection occurs in the enclosure. For $\beta = 0.1$ (Fig. 3(b)), the convection cell occurs in the region above the baffle and the fluid in the regions beside the baffle is virtually stagnant. As β increases further but less than $\beta^c = 0.51$ (Figs. 3(c)–(f)), the unicellular convection prevails and the convection is largely confined to the region above the baffle. As β increases beyond β^c (Figs. 3(g) and (h) for $\beta = 0.52$ and 0.6, respectively), the convection becomes bicellular where the baffle coincides with the dividing streamline of these two cells. Consequently, for $\beta > \beta^c$, the change of the baffle's height no longer has any influence on the stability characteristics.

To examine the influence of an off-centered baffle on the stability, three different enclosures with $\sigma = 0.5$, 1, and 2 are considered. Since the symmetry of the baffle's position with respect to the center of

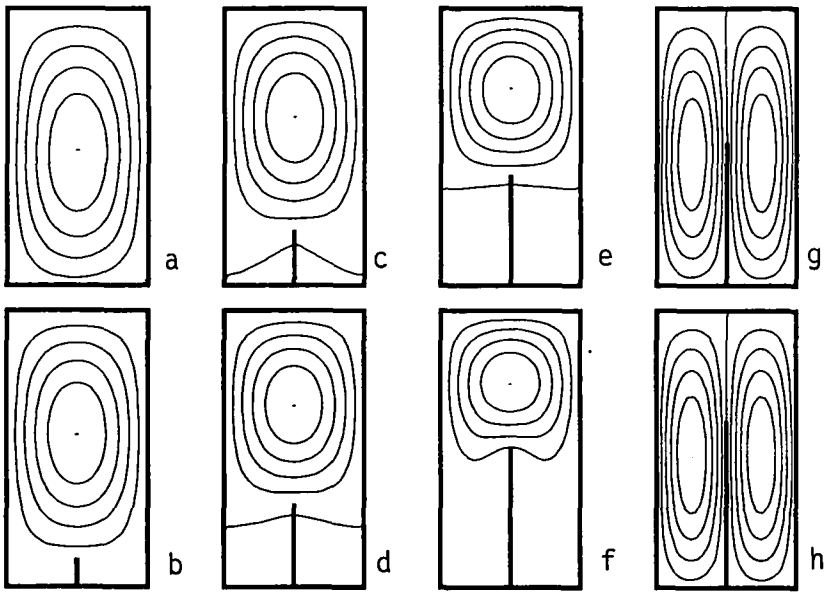

FIG. 3. Critical streamline patterns for various β when $\sigma = 0.5$ and $\lambda = 0.25$: (a) $\beta = 0$; (b) $\beta = 0.1$; (c) $\beta = 0.2$; (d) $\beta = 0.3$; (e) $\beta = 0.4$; (f) $\beta = 0.5$; (g) $\beta = 0.52$; (h) $\beta = 0.6$.

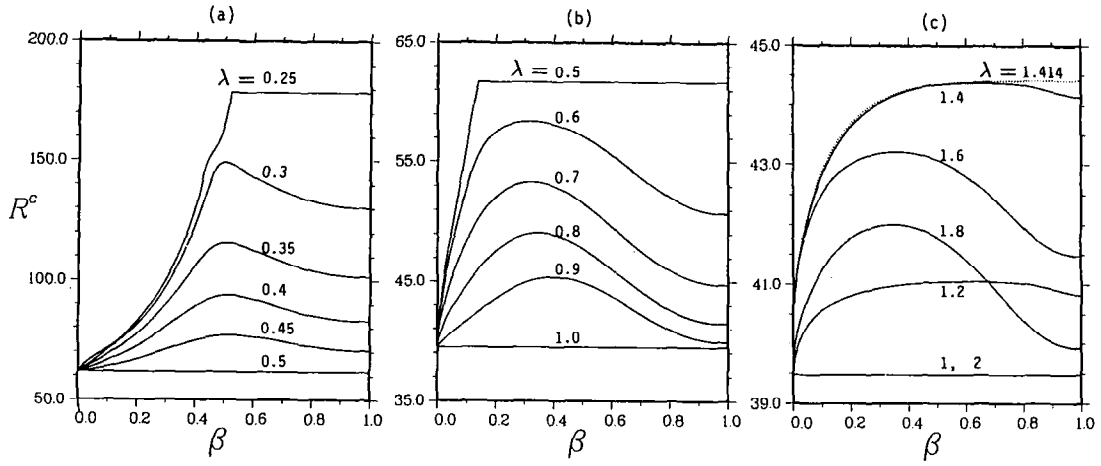

FIG. 4. Variation of R^c vs β for various λ: (a) $\sigma = 0.5$; (b) $\sigma = 1$; (c) $\sigma = 2$.

enclosure holds, we shall only consider the cases in which the baffles are placed in the right half of the enclosure, i.e. $0.5 \leqslant \lambda/\sigma \leqslant 1$. For $\sigma = 0.5$, the variations of R^c vs β for various λ are shown in Fig. 4(a). For $\lambda = 0.25$, a centered-baffle case, R^c increases monotonically with β first, reaches a constant at β^c and remains at the same value for higher β. For $0.25 < \lambda < 0.5$, off-centered baffle cases, R^c is a monotonically increasing function of β for $\beta < \beta^c$, which lies approximately at 0.51 for all σ considered, and becomes a decreasing function for $\beta > \beta^c$. For $\sigma = 1$, the variation of R^c vs β (Fig. 4(b)) shows a similar trend to that for $\sigma = 0.5$. The values of β^c for $\lambda = 0.5$, 0.6, 0.7, 0.8 and 0.9 are approximately 0.13, 0.31, 0.32, 0.33 and 0.41, respectively. For $\sigma = 2$, the situation becomes more complex. The R^c curves (Fig. 4(c)) show crossovers as λ varies. In general, the curves of R^c for $\sigma < \sqrt{2}$, in which the onset of convection is unicellular, tend to be flatter than those for $\sigma > \sqrt{2}$, in which a bicellular convection prevails. It is also found that the placement of the baffle at $\lambda = 1.414$ (more precisely, it should be $\sqrt{2}$) results in the most stable state compared with other cases considered. This is due to the fact that the critical streamline pattern is of largest aspect ratio compared with the other cases.

Again, we present the critical streamline patterns

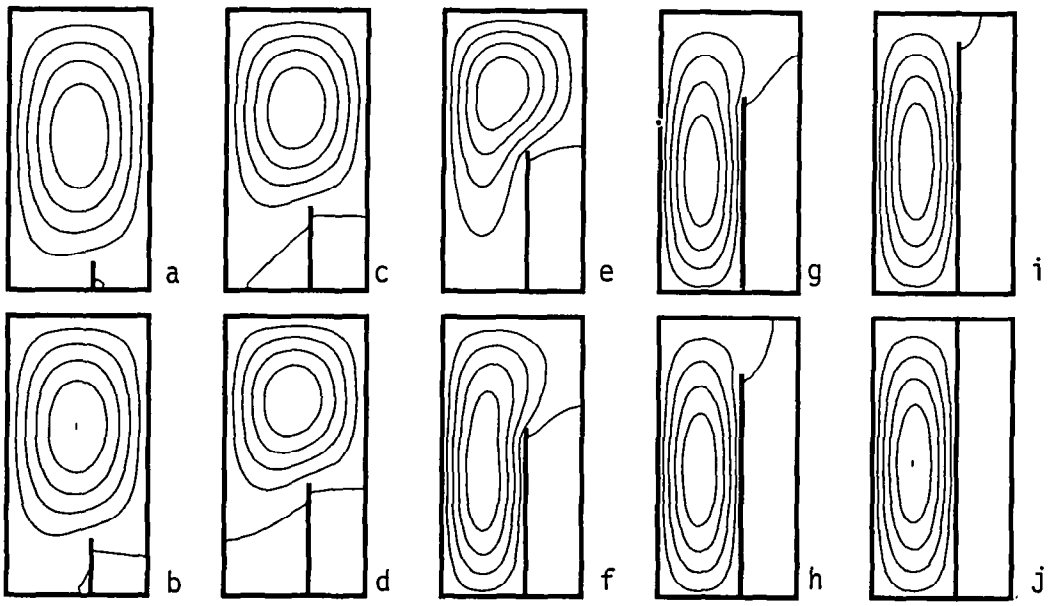

FIG. 5. Critical streamline patterns for various β when $\sigma = 0.5$ and $\lambda = 0.3$: (a) $\beta = 0.1$; (b) $\beta = 0.2$; (c) $\beta = 0.3$; (d) $\beta = 0.4$; (e) $\beta = 0.5$; (f) $\beta = 0.6$; (g) $\beta = 0.7$; (h) $\beta = 0.8$; (i) $\beta = 0.9$; (j) $\beta = 1$.

for $\sigma = 0.5$, $\lambda = 0.3$ in Figs. 5(a)–(j). In general, for $\beta < \beta^c$ ($=0.51$), the onset of convection occurs largely in the region above the baffle and, for $\beta > \beta^c$, the onset of convection mainly occurs in the left region, which has larger space and hence it is generally easier for the convection to set in. Near β^c (see Fig. 5(e) for $\beta = 0.5$), the convection cell appears to be in a transition mode between a high aspect ratio cell to a low aspect ratio cell. Physically, from the observation of R^c and the corresponding critical streamline patterns, it is found that a taller baffle does not necessarily result in a more stable state; moreover, it reveals that the most stable state is associated with the most crooked (least rectangular) critical streamline pattern, which is somehow more difficult to generate. That the stability does not increase with a taller baffle is due to the application of the Darcy model for the porous medium, in which the non-slip boundary condition on the rigid boundary cannot be prescribed. As a result, the change of critical streamline patterns due to varying baffle solely plays a crucial role in determining the stability characteristics.

From previous results, it is found that both the height and position of the baffle play decisive roles in determining the stability of the basic state of conduction. One also notes that the most stable state is associated with some particular values of λ, β, and σ. We shall thus in the following systematically seek the relations between these three parameters for which the most stable state may be obtained.

To examine the position of the baffle at which the most stable state occurs, we consider two enclosures of $\sigma = 3$ and 4 for $0 \leqslant \beta \leqslant 1$ and the results are shown in Figs. 6(a) and (b), respectively. For $\sigma = 3$ (Fig. 6(a)), there are two local maxima of R^c occurring at $\lambda = 1.5$ and 2.45 ($\approx\sqrt{6}$) for $\beta > 0$; wherein the R^c at $\lambda = 1.5$ is the largest. Physically, it means for an enclosure with aspect ratio $\sigma = 3$, a centered-baffle will lead to the most stable state while an off-centered baffle sitting at $\lambda = \sqrt{6}$, the second nodal value, results in the second most stable state. A baffle positioned at $\lambda = 2$, where the dividing streamline is located, results in the same stability ($R^c = 4\pi^2$) without the baffle; which, accordingly, corresponds to a most unstable state. For $\sigma = 4$ (Fig. 6(b)), the centered-baffle results in a most unstable state (because it overlaps the dividing streamline) whereas off-centered baffles located at the nodal values ($\lambda = \sqrt{6}$ and $\sqrt{(12)}$) correspond to the relatively most stable states; wherein the value R^c corresponding to $\lambda = \sqrt{6}$ is the largest. From Fig. 6, a conclusion can be reached that, despite varying β, the baffle's position corresponding to the most stable state is either at the center or at the nodal values. To illustrate this more precisely, the value of λ corresponding to the most stable state is summarized in Fig. 7, in which the horizontal segments of the curve correspond to centered-baffles and the inclined curves represent the baffles located at nodal values. The dotted lines serve merely as connecting lines between the horizontal segments and the inclined curves. Each dotted line is associated with a bifurcation point (lying, respectively, at $\sigma = 1.43$, 3.26, 5.20, 7.16 and 9.13) at which a centered-baffle leads to the same stability as that due to an off-centered baffle located at the nodal value.

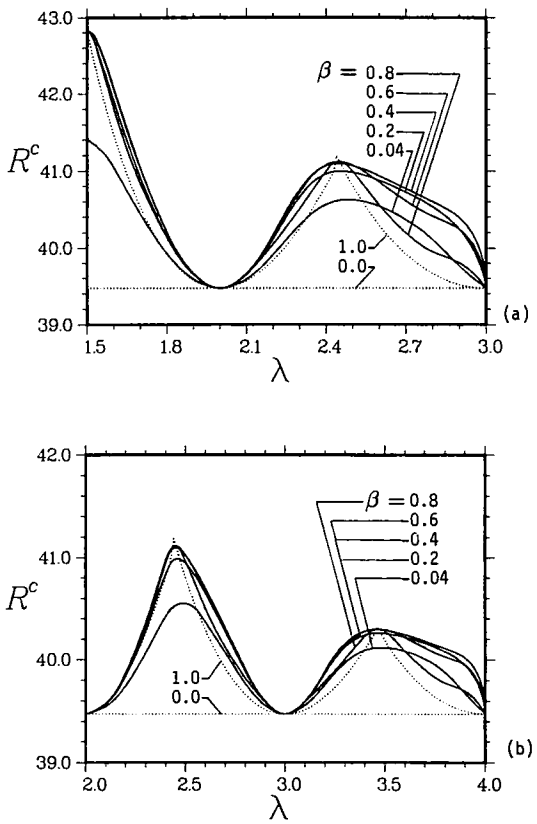

FIG. 6. Variation of R^c vs λ for various β: (a) $\sigma = 3$; (b) $\sigma = 4$.

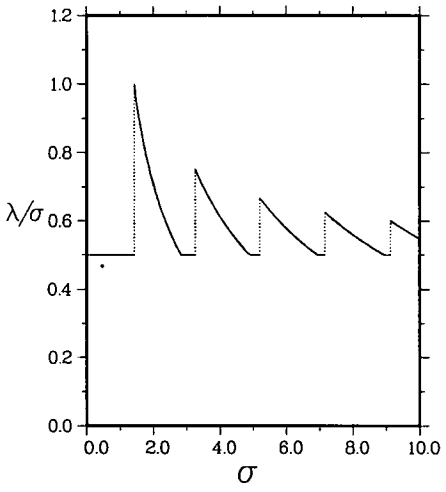

FIG. 7. The baffle's position in terms of λ/σ corresponding to the most stable state for enclosures with aspect ratio in $0 < \sigma \leqslant 10$.

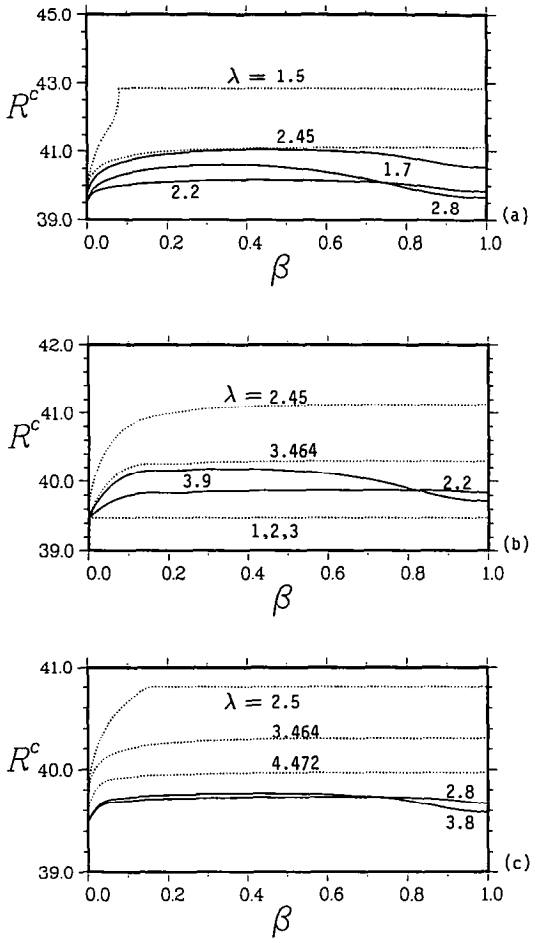

FIG. 8. Variation of R^c vs β for various λ: (a) $\sigma = 3$; (b) $\sigma = 4$; (c) $\sigma = 5$.

Table 1. The β^c and corresponding R^c for various λ and σ

σ	λ	β^c	R^c
0.5	0.25†	0.51 ~ 1	178.27
	0.30	0.51	149.07
	0.35	0.53	115.71
	0.40	0.53	93.68
	0.45	0.53	77.01
1.0	0.50†	0.13 ~ 1	61.68
	0.60	0.33	58.39
	0.70	0.33	53.33
	0.80	0.35	49.09
	0.90	0.41	45.37
2.0	1.00	0.00 ~ 1	39.48
	1.20	0.63	41.05
	1.40	0.67	44.38
	1.414†	1.00	44.42
	1.60	0.37	43.21
	1.80	0.35	42.00
3.0	1.50†	0.07 ~ 1	42.84
	1.586	0.47	42.24
	1.70	0.47	41.05
	2.20	0.47	40.18
	2.45	1.00	41.13
	2.80	0.35	40.61
4.0	2.00	0.00 ~ 1	39.48
	2.20	0.69	39.87
	2.45†	1.00	41.13
	2.586	0.41	40.75
	2.80	0.45	39.92
	3.20	0.43	39.89
	3.464	1.00	40.30
	3.70	0.35	40.18
5.0	2.50†	0.15 ~ 1	40.81
	2.55	0.52	40.68
	2.80	0.58	39.74
	3.20	0.52	39.73
	3.464	1.00	40.30
	3.586	0.41	40.19
	3.80	0.41	39.77
	4.20	0.41	39.76
	4.472	1.00	39.97
	4.60	0.40	39.95

† The λ for the most stable state of a particular σ.

As far as the baffle's height is concerned, we consider $\sigma = 3$, 4 and 5 and the variations of R^c vs β for various λ are shown in Figs. 8(a)–(c), respectively. In these figures, the dotted curves correspond to baffles located either at the nodal value or at the center and the solid curves to other cases. As one can see, the R^c for a centered-baffle (if it is not located on a dividing streamline) increases with β first, reaching a maximum, and remains at the same value for higher β. The R^c for an off-centered baffle located at the nodal value, however, is a monotonically increasing function of β and the maximum of R^c occurs at $\beta^c = 1$. For off-centered baffles located at non-nodal positions, R^c is an increasing–decreasing function of β and $0 < \beta^c < 1$. We tabulate in Table 1 the β^c and corresponding R^c for various λ and σ. It is found, quite interestingly, that for a particular σ, the β^c for the λ belonging to the same value of M are of approximately the same values. For instance, for $\sigma = 2$, the β^c for $1 < \lambda < \sqrt{2}$ (belonging to $M = 2$) are similar and so are those for $\sqrt{2} < \lambda < 2$ (belonging to $M = 3$). In addition, the β^c for the λ corresponding to the smaller M are generally larger than those of the larger M. In other words, an off-centered baffle located closer to the center needs to be taller in order to attain the most stable state than one located further from the center.

4. CONCLUDING REMARKS

From previous discussions, we can draw several conclusions concerning the influence on the stability in enclosures containing a fluid-saturated porous medium due to the presence of a vertical insulating baffle:

(1) The change of the stability due to the presence of a baffle is a result of the change of the onset convection patterns.

(2) Baffles at center or at nodal values correspond to a relatively more stable state.

(3) A taller baffle does not necessarily result in a more stable state. For a centered-baffle, the most stable state occurs for $\beta \geqslant \beta^c$, in which further increase of the baffle's height does not lead to any change in

stability. For an off-centered baffle located at a nodal value, the most stable state occurs at $\beta^c = 1$. For baffles at other positions, the most stable state occurs in the range $0 < \beta^c < 1$, where the values of β^c vary with λ but are similar to those of baffles located at positions within the same value of M.

As far as the engineering application is concerned, due to the fact that the aspect ratio σ affects significantly the stability in enclosures [12, 13], especially when σ is less than unity and the quiescent state becomes more stable, it is advantageous to partition the porous medium into tall, long regions so that a better insulation between top and bottom boundaries of the enclosure can be obtained. Instead of complete partitions which are expensive to build and install, according to the present results, the same or even better result of increasing stability can be achieved with partial baffles at a relevant position. A possible application of our results is in the design of the ceiling joists covered by a layer of insulation. The placement and size of the joists are currently determined only by structural requirements. Perhaps the joists may be redesigned to further serve as baffles to lower the heat loss through the ceiling.

REFERENCES

1. P. Cheng, Heat transfer in geothermal systems, *Adv. Heat Transfer* **14,** 1 (1978).
2. A. Bejan, Convective heat transfer in porous media. In *Handbook of Single Phase Convective Heat Transfer* (Edited by S. Kakac, R. K. Shah and W. Aung), Chap. 16. Wiley, New York (1987).
3. J. P. Caltagirone, Thermoconvective instabilities in a horizontal porous layer, *J. Fluid Mech.* **72,** 269 (1975).
4. R. N. Horne and J. P. Caltagirone, On the evolution of thermal disturbance during natural convection in a porous medium, *J. Fluid Mech.* **100,** 385 (1980).
5. P. H. Steen and C. K. Aidun, Time-periodic convection in porous media: transition mechanism, *J. Fluid Mech.* **196,** 263 (1988).
6. D. W. Stamps, V. S. Arpaci and J. A. Clark, Unsteady three-dimensional natural convection in a fluid-saturated porous medium, *J. Fluid Mech.* **213,** 377 (1990).
7. C. W. Horton and F. T. Rogers, Convective currents in a porous medium, *J. Appl. Phys.* **16,** 367 (1945).
8. Y. Katto and T. Masuoka, Criterion for onset of convection flow in a fluid in a porous medium, *Int. J. Heat Mass Transfer* **10,** 297 (1967).
9. R. J. Buretta, Thermal convection in a fluid filled porous layer with uniform internal heat sources, Ph.D. Dissertation, University of Minnesota, Minneapolis, Minnesota (1972).
10. F. Chen and C. F. Chen, Experimental investigation of convective stability in a superposed fluid and porous layer when heated from below, *J. Fluid Mech.* **207,** 311 (1989).
11. F. M. Sutton, Onset of convection in a porous channel with net through flow, *Physics Fluids* **13,** 1931 (1970).
12. J. L. Beck, Convection in a box of porous material saturated with fluid, *Physics Fluids* **15,** 1377 (1972).
13. D. E. Chelghoum, P. D. Weidman and D. R. Kassoy, The effect of slab width on the stability of natural convection in confined saturated porous media, *Physics Fluids* **30,** 1941 (1987).
14. A. Bejan, *Convective Heat Transfer*, Chap. 10. Wiley, New York. (1984).